

PEAK AMPLIFICATION AND BREAKUP OF A COHERENT OPTICAL PULSE
IN A SIMPLE ATOMIC ABSORBER

H. M. Gibbs and R. E. Slusher

Bell Telephone Laboratories, Murray Hill, New Jersey 07974

(Received 9 February 1970)

We report the low-loss propagation, peak amplification, and multiple breakup of a coherent laser pulse undergoing self-induced transparency by interacting with two nondegenerate levels of a highly absorbing gas of Rb atoms. These results are in good agreement with computer solutions of coupled Schrödinger and Maxwell equations including relaxation.

The low-loss propagation of a coherent light pulse through a highly absorbing medium of resonant two-level oscillators is known as self-induced transparency (SIT)¹ and has been observed in ruby¹ and a molecular gas.² We report here the first observations of this effect in a simple atomic system, the first clear demonstration of the breakup of a pulse undergoing SIT, and the first observation of peak intensity amplification by an absorber.

A simultaneous solution of Maxwell's equations, describing the effect of the atomic oscillators on the field, and Schrödinger's equation, giving the effect of the field on the atoms, predicts the lossless propagation of a pulse with electric field envelope¹

$$\mathcal{E}(z, t) = \frac{\hbar}{p\tau} \operatorname{sech} \left[\frac{1}{\tau} (t - z/V) \right], \quad (1)$$

where p is the electric dipole moment of the transition, τ is the final pulse width, and V is the pulse speed. Equation (1) describes what is called a 2π pulse because it rotates the effective macroscopic electric dipole moment through an angle

$$\theta \equiv \frac{2p}{\hbar} \int_{-\infty}^{\infty} \mathcal{E}(z, t) dt = 2\pi. \quad (2)$$

For $\theta = 2m\pi$ each atom of the ensemble undergoes m coherent transitions from ground to excited state and back to the ground state. Equation (1) can be obtained by assuming a coherent plane-wave pulse at exact resonance with a set of inhomogeneously broadened, lossless, nondegenerate, two-level absorbers. Computer solutions¹ with these assumptions but with input electric fields differing from (1) in shape or amplitude lead to the following predictions: (i) The energy E_0 transmitted through the absorber depends linearly upon the input energy E_I for $\theta \ll \pi$, i.e., $E_0 = E_I e^{-\alpha L}$ where α is the absorption coefficient and L is the cell length; increases much more rapidly than linearly in the region θ

$\approx \pi$; and is essentially equal to E_I for $\theta \gg \pi$.

(ii) The propagation velocity of the peak of the pulse is reduced (depending upon αL and θ) with a minimum for $\theta \approx \pi$. (iii) For $(2m-1)\pi < \theta < (2m+1)\pi$ the pulse evolves into m pulses (each with area $\approx 2\pi$). (iv) For some inputs, particularly for θ slightly less than 3π and 5π , the output peak intensity exceeds the input peak intensity. We have observed all of these predictions using a $^{202}\text{Hg}^+$ laser³ pulse at resonance with atomic ^{87}Rb absorption in a magnetic field. These results will be discussed after a description of the Hg-Rb system. Previous observations of SIT in ruby¹ and SF_6 gas² verified (i) and (ii) but did not see (iv) and only hinted at (iii) because one or more of the theoretical assumptions was violated.

In order to verify the above predictions quantitatively, the coherent optical pulse should have the following characteristics. First, for the theory to apply the major contribution to the frequency width of the pulse must arise from the Fourier transform of the pulse envelope and not from phase or frequency instabilities within the envelope. This was verified for the pulses used here by observing the frequency profile with a Fabry-Perot interferometer. This was achieved by operating the Hg II laser in a single transverse and longitudinal cavity mode.⁴ The difficulty of achieving such coherence with dye lasers has impeded their application to resonance problems. Second, the pulse should be a plane wave of uniform intensity profile. An output aperture is used here to approximate the uniform plane-wave condition. The nonuniform profile of most previous experimental beams has been ignored in comparing them with uniform plane-wave theories. Third, a stable coincidence with a good absorber is required. The absorber here is ^{87}Rb placed in a 74.5-kG magnetic field to shift the D_1 -line absorption from 7947.6 Å to the Hg II emission at 7944.6 Å. In spite of the large number of fixed-frequency laser lines it is difficult to find a coincidence with a good absorber. Both dye

and parametric lasers are tunable but difficult to frequency stabilize. Fourth, there must be sufficient power to reach the self-induced transparency region. For the transition used in Rb, a 2π square pulse of width $\tau_p = 7$ nsec corresponds to an intensity $c|\mathcal{E}_m|^2/4\pi = c\pi\hbar^2/4p^2\tau_p^2 = 2.8$ W/cm² for $p = 4.35 \times 10^{-18}$ esu cm.⁵ A peak intensity of about 25 W/cm² was used here.⁶

The following are the criteria for selecting an absorber assuming there exists a coincident laser. First, the absorber should be homogeneous with easily varied absorption coefficient α . Only gases meet this restriction in practice. The Rb α is easily controlled by the temperature. Second, the absorption transition should involve a unique dipole moment.^{1,7} A transition between two nondegenerate levels of ⁸⁷Rb is used.⁵ The lack of information on the angular momenta of the SF₆ levels is a serious drawback to that system. Third, the pulse length, τ_p , should be much longer than the inhomogeneous broadening time T_2^* , and much shorter than T_2 , the effective dephasing time of the induced dipole moment. $T_2^* \ll \tau_p$ ensures that the absorption coefficient is almost constant over the frequencies of the Fourier transform of the pulse. For the Hg-Rb system, $T_2^* = 0.8$ nsec from Doppler broadening, $\tau \approx 7$ nsec, and T_2 arises from the excited-state natural lifetime of 28 nsec. Collisional broadening is negligible at the densities $\approx 10^{12}$ cm⁻³ used here. Fourth, high absorption ($\alpha L > 3$) is required within a length for which the incident pulse can be approximated by a plane wave. This requires low diffraction loss, i.e., a Fresnel number $\eta = R^2/\lambda L$ greater than 1, where R is the radius of the region of uniform intensity and L is the cell length. Here $L = 1$ mm and $R < 60$ μ m depending upon the input intensity, so $\eta \leq 4.5$; in the region $\theta = \pi$, R may be much less than 60 μ m and diffraction losses appreciable. The Hg-Rb system is the first to satisfy all of the above criteria necessary for observing the predictions (i) to (iv).

The coherent optical pulse is generated by a pulsed Hg II laser operated at 160 Hz repetition rate. Diffraction losses of a small aperture eliminate all but the lowest order transverse mode. A thin Nichrome film selects a single longitudinal mode.⁸ The laser can be fine tuned within its 350- to 400-MHz gain curve by adjusting the voltage across a piezoelectric crystal stack to which the single mode selector is attached. The laser output is continually monitored with the aid of a stable (evacuated) Fabry-Perot inter-

ferometer. The mode-selector voltage is adjusted manually to keep the laser output within ± 50 MHz of the center of the absorption profile. The output of the laser passes twice through a Pockels cell to form the 6.5-nsec half-width pulses shown as dotted curves in Fig. 1. A quarter-wave plate after the Pockels cell converts the linearly polarized beam into either an absorbed right-circularly polarized or unabsorbed left-circularly polarized beam. Both polarizations were measured to be of equal intensity at the detector when the Rb vapor was tuned off resonance. A 38-cm lens is used to focus the beam to a plane wave front with Gaussian intensity profile of 115- μ m full width at the 1-mm-thick Rb cell in the center of a 74.5-kG superconducting solenoid (the Doppler inhomogeneous width was broadened by less than 5% by field inhomogeneities). The field and laser beam are parallel. The density is determined by the 80° to 100° cell temperature which is held to within 0.5°C. Radiation exiting from the cell is imaged with a magnification of 6.5 onto a 200- μ m aperture used to isolate a nearly uniform portion of the Gaussian profile beam. A large area T1XL59 silicon avalanche photodiode detects the pulse through the 200- μ m aperture with a time response of ≈ 0.3 nsec. The photodiode output is matched directly into a sampling oscilloscope. The traces shown in Fig. 1 were obtained by 60-sec sweeps of the sampling gate over the 20-nsec period of interest. A discriminator circuit accepted only pulses with $>95\%$ of the peak input intensity. The intensity of the pulse was decreased by delaying the Pockels-cell trigger with respect to the laser pulse, thus avoiding beam distortions and displacements.

At very low intensities the linear absorption for the data shown in Figs. 1 and 2 was measured to be $\alpha \approx 50$ cm⁻¹, i.e., $\alpha L = 5$. Figure 2 shows the output-to-input energy ratios as a function of the input energy with and without the 200- μ m aperture. First note that as predicted in (i) above, the energy ratio rises steeply to near unity at an incident intensity equal to that predicted by Eq. (2) within the accuracy of the power measurement ($\pm 50\%$). The effect of the Gaussian beam profile is to smooth out the sharp transition region as expected, because of the strong nonlinearity. Transverse scans of the output beam showed that the sides were "stripped" away when only the central intensity was large enough to form a 2π propagating pulse.

Characteristic output pulse shapes with the

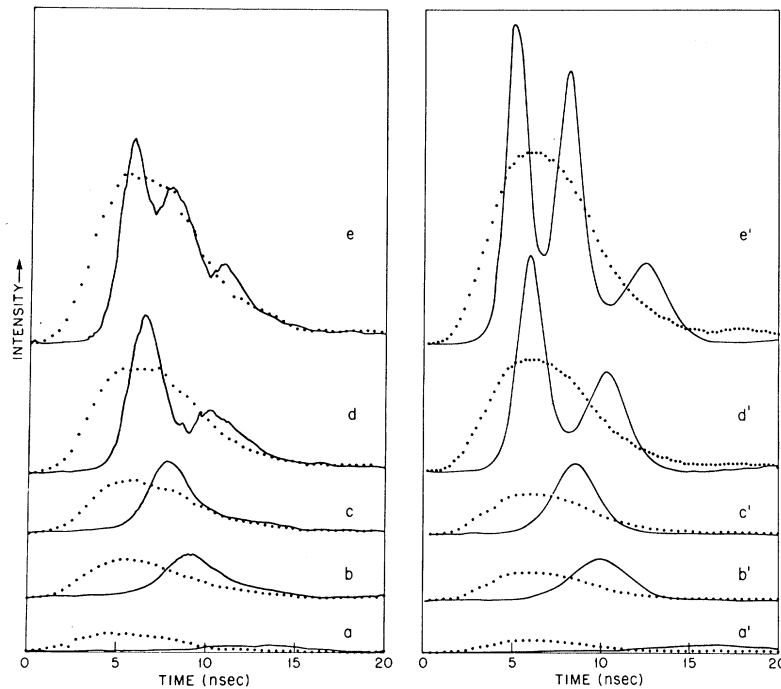


FIG. 1. Input and output optical pulse shapes. Sampling scope output and input pulses (obtained by rotating quarter wave plate through 90°) are shown in (a) through (e) corresponding to circled points in Fig. 2. Computer generated output pulses are shown in (a') through (e') corresponding to the circled points on the solid curve in Fig. 2.

corresponding input pulses are shown in Fig. 1. At low intensity the output was a highly attenuated replica of the input. As the energy ratio increased a delayed pulse was observed as in Fig. 1(a). The maximum observed delay of 15-20 nsec corresponds to a reduction in the propagation velocity to $\approx c/5000$ and a corresponding contraction in space from 2 m to a cigar shaped excitation region < 1 mm long in the Rb vapor. In (b) the pulse was delayed and reshaped to nearly the form of Eq. (1). At slightly higher input energy, (c), the output pulse peak intensity is clearly higher than the input, as predicted in (iv) above for a $\theta \approx 3\pi$ input pulse. For $4\pi < \theta < 5\pi$, a double pulse, (d), is obtained and, as predicted in (iii) above, the pulse broke into two 2π pulses. Finally in (e), for $\theta \approx 6\pi$, the pulse broke into three 2π pulses. Note that in the pulse-breakup region the output pulse peaked higher than the input. For $\alpha L \approx 6-7$ this peaking reached a maximum of $\approx 50\%$ higher than the output intensity for $\theta \approx 5\pi$. When the $200\text{-}\mu\text{m}$ output aperture was not used to isolate a uniform portion of the beam, the pulse breakup was smoothed out and the peak amplification was not observed.

We have obtained computer solutions of the coupled Bloch and Maxwell equations¹ including spontaneous emission from the excited state to the

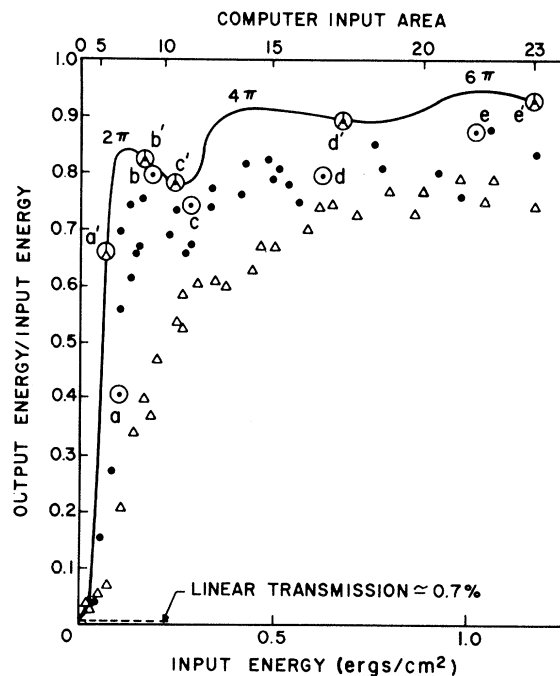


FIG. 2. Output-to-input energy ratio versus input energy. Solid curve is a uniform plane-wave computer solution. Solid dots are data taken with $200\text{-}\mu\text{m}$ output aperture to approximate uniform plane wave. Triangles are data with no aperture corresponding to a plane-wave input with Gaussian intensity profile.

absorbing state (partial lifetime $\tau \approx 42$ nsec) and to a third state ($\tau' \approx 84$ nsec).⁹ The computed output pulse shapes corresponding to those measured are shown in Figs. 1(a') through 1(e'). The corresponding computed energy ratios are shown in Fig. 2. The agreement between computed and experimentally observed pulse shapes and energy ratios is quite good considering experimental averaging such as diffraction losses in the region near $\theta \approx 2\pi$ and the time response and trigger jitter in the $\theta \approx 4\pi$ to 6π region.

The Hg-Rb system has been shown to be an excellent system for quantitative comparisons with SIT theory. Uniform intensity of the beam has been shown to be a necessity for observing peak amplification and pulse breakup. Further studies of off-resonance and focusing effects using the Hg-Rb system should be a valuable future contribution to this interesting interaction region.

We wish to acknowledge valuable discussions with S. L. McCall, and to thank C. C. Grimes for providing the superconducting solenoid. M. V. Schneider supplied the thin metallic film used as single mode selector. H. Melchior calibrated the time response of the photodiode and G. Churchill provided valuable technical assistance.

¹S. L. McCall and E. L. Hahn, Phys. Rev. Letters **18**, 908 (1967), and Phys. Rev. **183**, 457 (1969).

²C. K. N. Patel and R. E. Slusher, Phys. Rev. Letters **19**, 1019 (1967).

³The laser was constructed by Spectra Physics; see J. P. Goldsborough and A. L. Bloom, IEEE J. Quantum Electron. **5**, 459 (1969).

⁴The coherence time of the 1- μ sec Hg laser output is expected to be limited to several hundred nanoseconds by the 4-5% output through one end of the 280-cm cavity. A Pockels cell is used rather than a Kerr cell to extract a 5- to 10-nsec pulse because the former is expected to be free from the phase shifts of the latter (pointed out by S. L. McCall).

⁵The electric dipole moment p was calculated as follows. The Rb $5p^2P_{1/2}$ excited-state lifetime is 28.1 ± 0.5 nsec; J. K. Link, J. Opt. Soc. Am. **56**, 1195 (1966). At the operating field of 74.5 kG only the $M_I = \frac{3}{2}$ component of the right-circularly polarized absorption ($M_{J'} = M_J + 1$) is effective (the M_I components for ^{87}Rb are separated by 1.9 GHz compared with the 0.55-GHz Doppler width). But the excited state $M_J = +\frac{1}{2}$, $M_I = \frac{3}{2}$ substate spontaneously radiates to both the $M_J = -\frac{1}{2}$, $M_I = \frac{3}{2}$ and $M_J = +\frac{1}{2}$, $M_I = +\frac{3}{2}$ substates with a 2:1 branching ratio. For the 42-nsec partial lifetime and $(1/\tau) = \frac{4}{3}(\omega^3/\hbar c^3)p_s^2$ from L. I. Schiff, Quantum Mechanics (McGraw-Hill, New York, 1955), p. 261, one has $p_s = 6.16 \times 10^{-18}$ esu cm, but in the notation of McCall and Hahn, $p = p_s/\sqrt{2}$. The transition to the $M_J = +\frac{1}{2}$, $M_I = \frac{3}{2}$ substate means that this is only approximately a two-level system; however, the third level is included in computer simulations.

⁶The single-mode peak power of the laser's 1-mm-diam output beam was measured to be 0.1 to 0.2 W. The intensity at the cell was then determined by measuring transmission losses and the beam profile at the cell.

⁷C. K. Rhodes, A. Szöke, and A. Javan, Phys. Rev. Letters **21**, 1151 (1968).

⁸P. W. Smith, M. V. Schneider, and H. G. Danielmeyer, Bell System Tech. J. **48**, 1405 (1969).

⁹Previous computations [Ref. 1 and F. A. Hopf and M. O. Scully, Phys. Rev. **179**, 399 (1969)] have not treated spontaneous relaxation between the SIT levels correctly.